General approach to the nucleation and crystal growth in $Sb_{0.5}Se_{99.5}$ glass explaining shape of DSC curves

P. Honcová[1*], J. Shánělová[2], J. Barták[2], J. Málek[2], P. Koštál[1], S. Stehlík[1]

[1]Department of Inorganic Technology, University of Pardubice, Doubravice 41, 53210 Pardubice, Czech Republic

[2]Department of Physical Chemistry, University of Pardubice, Studentská 573, 53210 Pardubice, Czech Republic

Keywords: crystallization kinetics; Sb-Se; crystal growth rate; nucleation rate; overlapping peaks; chalcogenide glasses

Abstract

Crystallization of amorphous $Sb_{0.5}Se_{99.5}$ glass in the form of bulk and powder with defined particle sizes (prepared in protective atmosphere of argon) was studied by DSC. Different forms of sample exhibit quite complex behaviour involving crystallization on the surface and in the volume of the sample and it is reflected in the shape of DSC curve. Standard kinetic analysis cannot describe experimental results with interpretation of crystal growth mechanism, although the deconvolution procedure was done using several kinetic models, because of the time-lag of crystallization in the volume. However, theoretical curves based on nucleation and crystal growth rates, calculated separately for the process on the surface and in the volume of the sample, well correspond to real data and explain distinctive change in the shape of DSC curves with particle sizes.

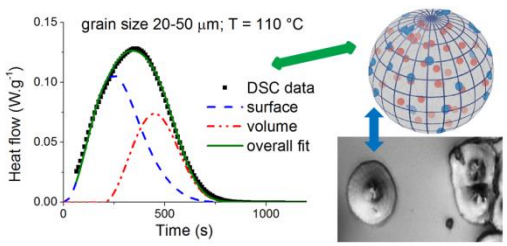

*Corresponding author, e-mail: pavla.honcova@upce.cz; tel. No. +420466037179

Introduction

Chalcogenide materials are in the centre of interest for many decades because of their properties and application in various solid-state devices. The Sb–Se glasses are attractive candidates for applications such as data recording devices requiring low melting temperatures, low thermal conductance and high viscosity.[1,2] The application of chalcogenide glasses based on amorphous or amorphous-crystalline changes requires the knowledge of crystallization process and thermal stability. The crystallization studies focus on the determination of nucleation and crystal growth mechanism and kinetics[3-5] to be able to predict the crystallization behavior under various conditions. Appropriate prediction of crystallization process allows controlling and optimizing of conditions for new high-tech material production. Crystallization behavior can be studied directly by observing of crystals growing in material under specific conditions[4,6] or indirectly by monitoring specific properties of studied material[3,7-9]. The direct observation of crystal growth is very time consuming, thus the indirect methods are preferred. Classical techniques for studying overall crystallization in glasses are differential scanning calorimetry (DSC) and differential thermal analysis (DTA) that have been developed over past 40 years. Analysis of the experimental data obtained from the both methods (DSC and DTA) enables to estimate the crystallization mechanism and kinetics.

The output signal of DSC is a heat flow, Φ, dependent on time (isothermal conditions) or temperature (non–isothermal conditions) and it can be expressed[10] as:

$$\Phi = \Delta H \cdot \left(\frac{d\alpha}{dt}\right) \quad (1)$$

where ΔH is the enthalpy change of the process, α is the conversion, and t is the time.

The mathematical modeling of DSC signal includes kinetic parameters describing studied process, so the heat flow can be described[10] as:

$$\Phi = \Delta H \cdot A \cdot e^{-E/RT} \cdot f(\alpha) \quad (2)$$

where A is the pre-exponential factor, E is the activation energy of the process, R is the universal gas constant, T is the temperature, and $f(\alpha)$ is the kinetic model. In the case of chalcogenide glasses, the frequently used model describing crystallization is nucleation-growth model formulated by Johnson and Mehl[11] and Avrami[12] giving the following expression (referred to as JMA):

$$f(\alpha) = n(1-\alpha)[-ln(1-\alpha)]^{1-1/n} \quad (3)$$

where the kinetic exponent *n* depends on the crystal growth morphology[13]. The validity of the JMA equation[14-16] is based on the following assumptions: (i) isothermal crystallization conditions, (ii) homogeneous nucleation or heterogeneous nucleation at randomly dispersed second-phase particles, (iii) growth rate of new phase independent of time, and (iv) low anisotropy of growing crystals.

The procedure of kinetic analysis of a single peak is well known[10,16], where the determination of activation energy is followed by selection of appropriate kinetic model and after that parameters of selected model are determined. Several kinetic models and their parameters are related with the concept of crystal growth mechanism[10,13]. In the case of overlapping peaks, the full kinetic analysis can be performed after the deconvolution process, which can be done by numerical fitting using a general equation describing various shapes of DSC peaks such as Fraser–Suzuki function (only for non–isothermal conditions)[17-19] or deconvolution based on selected function[20-22]. The analysis of overlapping DSC or DTA peaks, without deconvolution, can be done partially when only the value of activation energy is determined from non–isothermal measurements[23-25] but the information about crystal growth morphology and mechanism is missing. However, some papers include deconvolution procedure followed by full kinetic analysis[26-28]. Nevertheless, deconvolution of data obtained under isothermal conditions[5,29] can be performed using selected kinetic model, which can significantly influence the interpretation of mechanism of crystallization. As mentioned above, the JMA model and its parameter provide the information about the mechanism of crystallization. However, this information corresponds to reality only when JMA model is suitable to described the data, i.e. when the assumptions of JMA model are fulfilled (it will be discussed later).

In the case of antimony-selenium system, the amorphous material can be produced by conventional method only with less addition of antimony into selenium. Crystallization in Sb–Se system observed by differential scanning calorimetry (DSC) indicates the presence of overlapping peaks caused by crystallization of Sb_2Se_3 and crystallization of Se on the surface and in the volume of studied samples[21,30]. However, some authors observed only single peak[31,32]. So, one of the main aim of this work was to performed extended study of crystallization in Sb-Se system with low addition of antimony.

Furthermore, the general attitude to DSC method is that it is easy to carry out; it requires little sample preparation; it is quite sensitive, and it is relatively independent of

sample geometry[32]. This work shows that this meaning about DSC is true except underestimation of sample geometry influence (means the shape of studied sample, i.e. powder, bulk). Data presented in this work emphasized the importance of the form of studied sample and its influence on interpretation of crystallization mechanism. Moreover, the different sample form can reveal the complex character of studied process which was for $Sb_{0.5}Se_{99.5}$ composition described by new kinetic model based on nucleation and growth rate curves.

Experimental

The amorphous $Sb_{0.5}Se_{99.5}$ material was prepared from pure elements (5N, Sigma Aldrich) by conventional method: pure elements were weighted into quartz ampoule, ampoule was evacuated and sealed, and then put into rocking furnace, where the melting and homogenization was performed at temperature 800 °C for 20 hours and consequently at 600 °C for 4 hours; then the ampoule was quenched in cold brine. Two batches of samples were prepared in order to check the reproducibility. When the total amount of weighted elements was only 4 g and during the cooling the thin layer of the melt in the ampoule was created, only then the prepared material was amorphous (otherwise partially crystalline material was obtained). The amorphous nature of prepared sample was confirmed by X-ray analysis as well as by scanning electron microscopy (SEM) and by using optical and infrared microscopy. The composition of prepared glass was check by EDAX microanalysis.

All samples for DSC analysis were prepared under protective atmosphere of argon, i.e., from the breaking of the ampoule to the closing of the sample into the hermetically sealed aluminum pan for DSC analysis, the manipulation with the sample was done in protective glove-box filled with argon. Amorphous samples were in the form of bulk (thin plate without any surface treatment) and powder with particle size of 20–50, 125–180 and 300–500 μm were prepared by crushing of bulk sample in agate mortar and consequent separation using sieves. The crystallization was studied under isothermal conditions using differential scanning calorimeter (DSC) Pyris 1 with intracooler 2P (Perkin-Elmer). The melting temperatures of several pure metals (Hg, Ga, In, Sn, Pb, and Zn) were used to calibrate temperature and the enthalpy was calibrated using enthalpy of fusion of indium. The samples were weighted into aluminum pans and empty pan was used as a reference. The

sample mass was circa 10 mg and the protective atmosphere of dry nitrogen with the flow rate of 20 cm^3 min^{-1} was used. The isothermal measurements of the samples were done in the temperature range from 95 °C to 117 °C for the time necessary to finish the crystallization process when the temperature of isotherm was reached by heating from 20 °C by rate of 150 °C min^{-1}. DSC curves obtained for different sample forms or different temperatures are illustrated in Figures 1 and 2. The glass transition temperature (T_g) of prepared $Sb_{0.5}Se_{99.5}$ glass was determined by heating the bulk sample by the rate of 20 °C min^{-1} when the previous thermal history was firstly erase by heating the sample to temperature well above T_g and subsequently the sample was cooled down to temperature -10 °C by rate of 20 °C min^{-1}. The glass transition temperature is 41 °C (determined as a mid-point).

The standard kinetic analyses with deconvolution were done using software OriTas[33] utilizing conventional kinetic models. The calculations are based on the standard kinetic equations and the appropriate model describing experimental data is selected on the base of characteristic functions introduced by Málek[10]. In the case of our DSC curves different modulus of OriTas software were used to estimate values of parameters describing both peaks and select the kinetic model. Then these preliminary parameters and models were specified in the modulus for deconvolution to obtain the best simulation of experimental data. The overall curve was calculated as a sum of two peaks and the best result was the best fit of data by the overall curve. The models used for data description were JMA (given by Equation 3) with parameter *n* and Gaussian curve with three parameters expressed as:

$$f(x) = Y \cdot e^{-\frac{(x-X)^2}{2w^2}} \quad (4)$$

where *Y* is the height of the curve's peak, *X* is the position of the center of the peak and *w* is the width of the “bell”.

The simulation and fitting of experimental data was also done using new kinetic model based on nucleation and crystal growth rates (described later).

The crystallization was directly observed by microscope Olympus BX51 equipped with an infrared XM 10 camera in reflection mode. The sample in the form of bulk was previously heat treated at temperature of 104 °C for different time in a computer-controlled furnace (central hot zone was constant within ±0.5 °C), and after the annealing the samples were

rapidly cooled down to the room temperature. After that the samples were broken or polished to observe both surface and bulk crystallization.

Results and discussion

The amorphous $Sb_{0.5}Se_{99.5}$ material in the form of bulk and powder with defined particle sizes was prepared under protective atmosphere of argon and studied using DSC under isothermal conditions. Testing of crystallization in $Sb_{0.5}Se_{99.5}$ material with different particle size samples brings DSC peaks significantly different in their shape. In all cases, the decreasing temperature of isotherm caused shift of crystallization peak to longer time as is shown in Figure 1. At the same time, decreasing particle size shifts main part of crystallization peak to shorter annealing time. However, Figure 2 shows that the crystallization peak for particle size of 300–500 μm takes a bit longer time than bulk sample. DSC response of the lowest particle size of 20–50 μm samples (Figures 2 and 4) can be considered as a single peak, although for lower temperatures there is a broad maximum of measured crystallization peak (especially for the temperature of 102 and 97 °C). Samples with particle size of 125–180 μm show very broad peak in its maximum leading to nearly two distinct maxima (Figure 1). Particle size of 300–500 μm displays clear shoulder on the beginning of the crystallization peak but the main peak has narrow maximum. Similarly, the bulk sample exhibits narrow main peak, nevertheless there is almost separated first effect on the beginning of the crystallization effect. For bulk sample and annealing temperature of 97 °C, there is only slowly increasing heat flow on the beginning of crystallization peak. The illustration of the peak shift with annealing temperature and effect of particle size is given in Figures 1 and 2. The overall measured enthalpy change of crystallization process is about 49 J g^{-1} for bulk sample and sample of particle size 300–500 μm, lower value of 46 J g^{-1} was obtained for particle size of 125–180 μm, and the lowest is the enthalpy change for particle size of 20–50 μm equals to 41 J g^{-1} (typical experimental error does not exceed 10%).

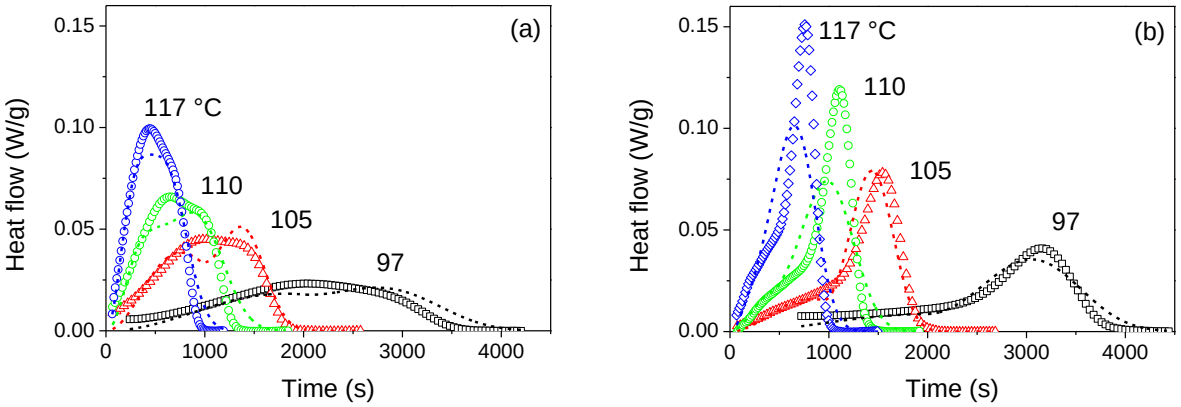

Figure 1 The set of DSC data obtained for given temperatures and samples in the form of powder with particle size (a) 125–180 μm and (b) 300–500 μm. The symbols correspond to experimental data and dashed lines correspond to data calculated using parameters summarized in Table 2.

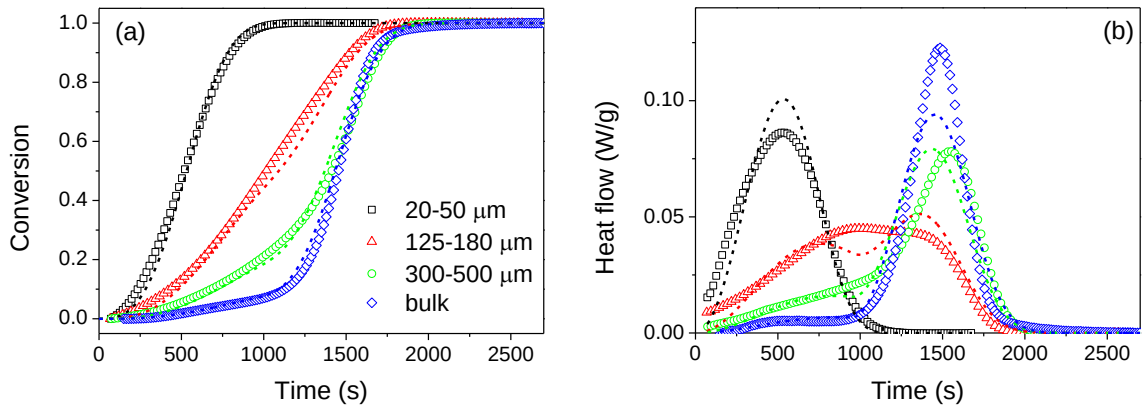

Figure 2 The set of DSC data obtained for samples with different particle size tested at temperature 105 °C. The symbols correspond to experimental data in the form of conversion or heat flow and dash lines correspond to data calculated using parameters summarized in Table 2.

The phase diagram of Sb–Se system[34,35] clearly indicates that in composition with 0.5% of antimony, the crystal phase consists of Sb_2Se_3 and selenium. It is known that crystallization of selenium includes crystals growing on the surface and in the volume of the sample[36-38]. Thus, three overlapping DSC peaks are expected. However, the amount of 0.5 % of antimony and corresponding amount of Sb_2Se_3 crystals seem to be negligible in total

crystallization process. There is also no evidence of corresponding crystallization peak on DSC curve or any indication in X-ray diffractogram of completely crystallized sample. Therefore, creation of crystals with Sb is neglected in further analysis of experimental data. Comparing the experimental data with published results for pure selenium, it is evident that the shape of DSC peaks is different. In the paper of Svoboda and Málek[38], the isothermal crystallization of pure selenium was studied for samples with different particle sizes and in their paper there is a heat flow dependence on time depicted for sample with particle size of 125–180 μm. DSC data published by these authors exhibit right on the beginning steep slope with sharp maximum followed by slowly decreasing signal. Comparing the mentioned to the data given in Figure 1, we can conclude that the addition of antimony somehow hold the beginning of the crystallization process up, which results in slower evolution of the heat at the beginning of studied process. However, our data were obtained for samples prepared under inert atmosphere, which can influence the shape of the peak and the duration of crystallization process similarly as was observed for Sb_2S_3–GeS_2 glass[39]. Nevertheless, the time necessary to finish the crystallization process at given temperature is roughly comparable for pure selenium[38] and our data.

As was previously mentioned, the DSC peaks of particle size 20–50 μm can be considered as a single peak. And that is the reason why we can find papers describing crystallization in Sb–Se system using the standard kinetic analysis of single peak –these crystallization studies were performed on samples in the form of fine powder[31,32] (there are no information about particle size of studied samples). Increasing particle size of studied $Sb_{0.5}Se_{99.5}$ samples caused that the DSC peak became broader with clear evidence of complex crystallization process (see Figures 1 and 2). In this case, the kinetic analyses of overlapping peaks must be applied as described in the Introduction. Performing data analysis by the deconvolution process followed by kinetic analysis, as described in Reference[21], leads to results summarized in Table 1. All the data can be described using two overlapping peaks; illustration is given in Figures 3a and 4a. The same value of activation energy (summarized in Table 1) was used for both separated processes. The value of *E* decreases with increasing particle sizes and is a bit lower than values published for selenium in reference [38]. The first deconvoluted process is calculated using JMA model with parameter in the range of 2.2–2.9 indicating mechanism of two- or three-dimensional growth, respectively. The second peak is calculated for low particle sizes using JMA model too but the symmetric Gaussian function

must be applied to fit well the experimental data for bulk and the highest particle size samples. Similar result of deconvolution process was also obtained for Sb_2Se_{98} material[21]. Nevertheless, the application of Gaussian function does not contribute to the interpretation of crystal growth mechanism and does not even explain huge difference in the shape of DSC curves with particle size. Moreover, the value of kinetic exponent of JMA model for samples with lower particle sizes is 4 and higher, which is too high for chalcogenide material and is almost on the limit of believable value connected with crystal growth mechanism[10,13]. Further, the deconvoluted peaks illustrated in Figure 4a for the lowest particle size indicate that the surface crystallization has the same extent as the crystallization in the volume (the area of both deconvoluted peaks is similar, i.e. similar value of ΔH in Table 1) which is improbable for such a low particle size. The impossibility of fitting all the data with standard kinetic model and its reliable parameters is a consequence of basic assumption that the process starts right on the beginning of the annealing the sample, which will be discussed later.

Table 1 Values of parameters describing crystallization of $Sb_{0.5}Se_{99.5}$ samples obtained by kinetic analysis of overlapping peaks; activation energy of both effects *E*, enthalpy change $\Delta H_{1,2}$ of the first or the second peak, parameter of JMA model *n* (see Equation 3), and parameters of Gaussian function (see Equation 4): position of the center of the peak *X*, height of the curve's peak *Y*, and width of the "bell" *w*.

sample	*E* (kJ mol^{-1})	1st effect		2nd effect				
		ΔH_1 (-J g^{-1})	n_1	ΔH_2 (-J g^{-1})	n_2	Gaussian function		
						X (s)	*Y* (W g^{-1})	*w*
Bulk	65	10±2	2.5±0.2	41±6	-	1606±677	0.13±0.05	161±56
300-500 μm	73	24±2	2.9±0.2	25±4	-	1641±914	0.08±0.03	169±79
125-180 μm	85	35±4	2.4±0.1	17±3	4.7±0.1	-	-	-
20-50 μm	88	28±1	2.2±0.2	24±3	3.7±0.1	-	-	-

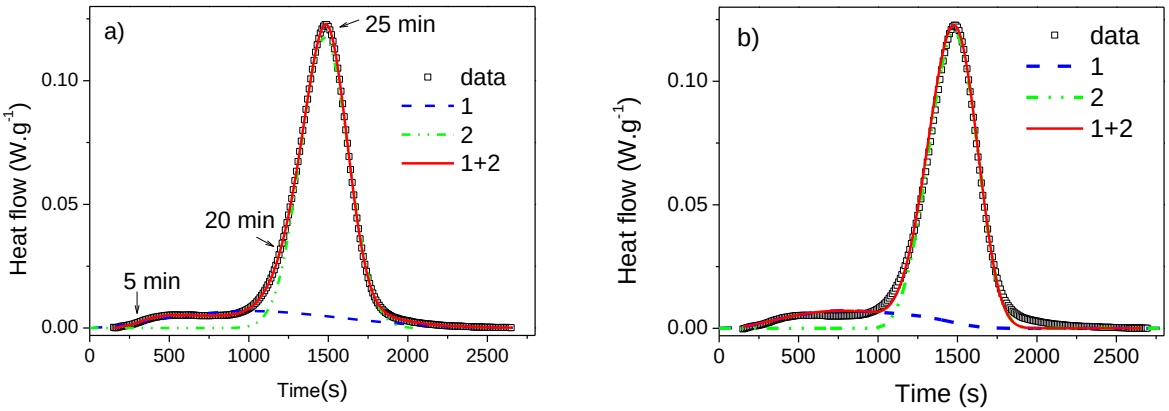

Figure 3 Deconvolution (a) by "standard" procedure (using JMA model and Gaussian function) and (b) based on simple model of nucleation and growth as a best fit of experimental data for bulk sample crystallized at temperature of 105 °C. In both cases, the parameters are relatively close to average values summarised in Tables 1 and 2. Arrows in (a) emphasize the annealing time of sample observed by microscopy and corresponding to photos illustrated in Figure 5.

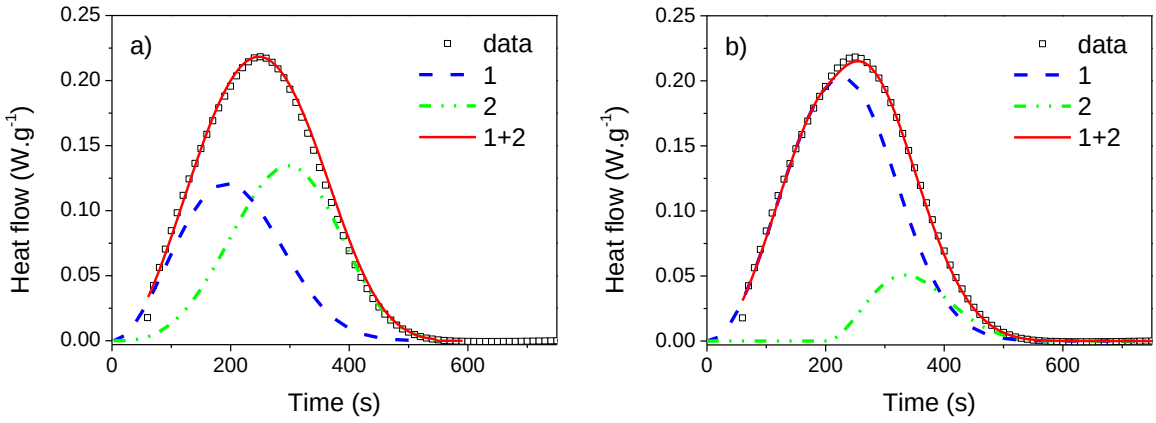

Figure 4 Deconvolution (a) by "standard" procedure (using JMA model for both peaks) and (b) based on simple model of nucleation and growth as a best fit of experimental data for sample with particle size of 20–50 μm crystallized at temperature of 117 °C. In both cases, the parameters are relatively close to average values summarised in Tables 1 and 2.

The direct observation of crystal growth was done using bulk sample annealed at temperature of 104 °C for different time; the illustration is given in Figure 5 and given annealing times are emphasized on DSC curve shown in Figure 3a. The detail of growing

crystals confirmed that spherulites of selenium are formed similar to that described by Ryschenkow and Faivre[4] and by Barták[40]. The low concentration of antimony in $Sb_{0.5}Se_{99.5}$ composition caused that any presence of Sb_2Se_3 crystals was not observed. It is evident that the crystallization process does not start at the same time on the surface and in the volume of $Sb_{0.5}Se_{99.5}$ sample. The direct observation showed that the crystallization on the surface starts first where no crystals can be found in the volume up to annealing time of 15 minutes. Then the layer of the crystals on the surface grows and some crystals occurred in the volume. Finally, the layer formed by the crystals on the surface still grows as well as crystals in the volume.

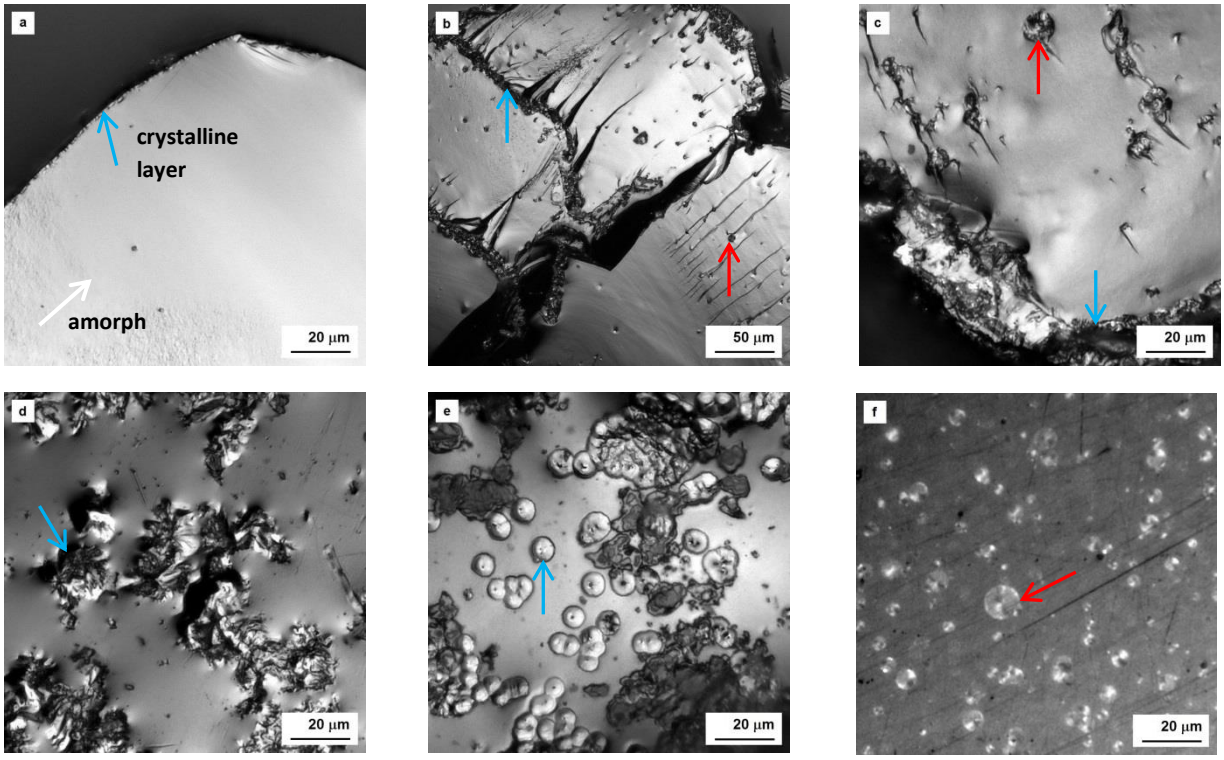

Figure 5 Sample surface and volume morphology observed by IR microscopy. Sample annealed at 104 °C for (a, d) 5 minutes; (b, e) 20 minutes; and (c, f) 25 minutes. Detail of the surface is given in (d, e); detail of the volume is given in (a, b, c, f). Figure (f) shows polished sample. The arrows emphasized the observed phase: white is for amorphous phase, blue for crystals on the surface and red for crystals in the volume. The dark "strikes" visible in (b) and (c) result from the breaking of the studied samples to observe the bulk crystallization using the microscopy.

The illustration of observed crystallization is given in Figure 5, where the crystals growing on the surface are emphasized by blue arrows and crystals growing in the volume by red arrows. The spherical particles in Figure 5d and e are the crystals formed on the surface of the sample which are continuing growing and finally fulfil the whole surface and then continue in growing as a compact crystalline layer. The crystals on the surface grow from the surface into the volume of the sample but under some circumstances upturned spherulites can be observed (Figure 5e shows detail of upturned spherulites of selenium growing on the surface of the sample).

This time-lag of the crystal growing in the volume of the sample explains why the JMA model cannot successfully describe DSC curves during deconvolution – one of the assumptions of JMA model is that the nucleation and growth starts immediately on the annealing.

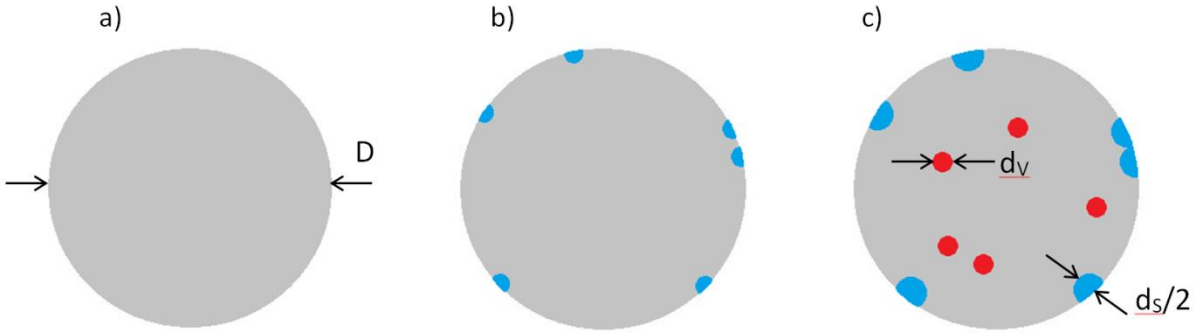

Figure 6 Illustration of grain of (a) amorphous material. Crystallization process starts (b) with crystals developing on the surface followed by (c) their growing together with crystals occurred in the volume of the grain. The diameter *D* of the grain, d_S and d_V of the crystals on the surface and in the volume are depicted.

Simple nucleation-growth rates model

According to the previous paragraphs, the fitting treatment based on simple concept covering nucleation and growth process on the surface and in the volume of the sample was proposed. As mentioned above, the crystallization of Sb_2Se_3 is neglected and only crystallization of selenium on the surface and in the volume is considered. The basic assumption is that the sample is a sphere with the diameter equal to 1 mm for bulk and is

equal to the average value calculated for low and high particle size limit (i.e., for sample with particle size in the range of 20–50 μm, the average value is 35 μm; diameter *D* of the grain in Figure 6) in the case of powder samples. Another assumption is that the nucleation and growth of the crystals on the surface and in the volume is independent of each other, but there is a uniform size of the crystals on the surface (diameter of the crystal d_S, see Figure 6) and uniform size of crystals in the volume of the grain (diameter of the crystal d_V, see Figure 6). Furthermore, the crystallization process does not have to start immediately but there could be a time-lag (τ_S for surface crystallization and τ_V for volume crystallization, respectively). The simplest shape of the crystals was chosen: on the surface a hemisphere grows, whereas in the volume it is a sphere. The shape of growing crystals corresponds to direct observation of crystallization in selenium[4,40]. The volume of one crystal V_i on the surface (subscript *S*) and in the volume of grain (subscript *V*) is:

$$V_{iS} = \frac{2}{3}\pi\left(\frac{d_S}{2}\right)^3 \quad (5)$$

$$V_{iV} = \frac{4}{3}\pi\left(\frac{d_V}{2}\right)^3 \quad (6)$$

The sizes of crystals are given by crystal growth rates on surface u_S and in volume u_V of the sample (the unit of the rates is m s^{-1}) at given temperature *T* and time period between time *t* and time-lag τ. Diameter of crystals on surface and in volume can be expressed as:

$$d_S = u_S(t - \tau_S) \quad (7)$$

$$d_V = u_V(t - \tau_V) \quad (8)$$

The time-lag is caused by the nucleation process. On the base of experimental observations we suppose that the most nuclei are created in a short time period near time-lag. Therefore, the simple model of crystallization supposes constant number of crystals on the surface of the grain N_S and in the volume of the grain N_V created in time τ_S or τ_V, respectively.

However, the growing crystals interfere in each other, so the volume of crystalline phase must be lower than the sum of crystal volumes. The impingement of crystals can be solved as a stochastic problem. The probability P_i of occurrence of non-crystalline phase after creation of one crystal (volume V_i) on/in the grain (volume *V*) is given as ($1-V_i/V$). Each crystal has the same probability, so the global probability is their multiplication. Thus, the conversion of the process can be expressed as (the equation was verified by Monte-Carlo simulation):

$$\alpha = 1 - \left(1 - \frac{V_i}{V}\right)^N \quad (9)$$

The conversion corresponding to the surface and volume crystallization is calculated separately, but there are not independent. The surface crystallization is localized in a surface spherical layer with the thickness $z_S = d_s/2$. The volume of the grain available for surface crystallization can be expressed as:

$$V_S = \frac{4}{3}\pi\left[\left(\frac{D}{2}\right)^3 - \left(\frac{D}{2} - z_S\right)^3\right] \quad (10)$$

Finally, the general expression of conversion given by equation (9) can be calculated for surface crystallization including Equations (5, 7, 10) and giving the form:

$$\alpha_S = 1 - \left(1 - \frac{V_{iS}}{V_S}\right)^{N_S} \quad (11)$$

The volume of crystals on the surface can be then expressed as:

$$V_{S,cr} = V_S \cdot \alpha_S \quad (12)$$

The volume of the grain available for volume crystallization covers also the non-crystalline space on the surface and can be calculated as:

$$V_V = \frac{4}{3}\pi\left(\frac{D}{2} - z_S\right)^3 + V_S(1 - \alpha_S) \quad (13)$$

Thus, the conversion corresponding to the volume crystallization has the form similar to equation (11) for surface crystallization and can be written as:

$$\alpha_V = 1 - \left(1 - \frac{V_{iV}}{V_V}\right)^{N_V} \quad (14)$$

The volume of crystals in the volume of the grain can be expressed as:

$$V_{V,cr} = V_V \cdot \alpha_V \quad (15)$$

Finally, the total volume of the crystals on/in the grain V_{cr} is a sum of $V_{S,cr}$ and $V_{V,cr}$. Thus, the overall conversion is given by the ratio of crystalline volume to the volume of the grain as:

$$\alpha = \frac{V_{cr}}{V} \quad (16)$$

The heat flow corresponding to the overall conversion can be calculated based on Equation (1), where the value of ΔH is determined from DSC data and the derivation of overall conversion (given by Equation (16)) and time is solved numerically. The fitting procedure compares this theoretical data with experimental where the fitting parameters are the number of particles per mm^2 (N_S), the crystal growth rate (u_S), and the time-lag (τ_S) for the surface; and the number of particles per mm^3 (N_V), the crystal growth rate (u_V), and the time-lag (τ_V) for the volume.

The correlation of surface/volume crystallization reflects in the whole set of data for samples with different particle sizes studied at selected temperature, which was fitted at once and obtained parameters are summarized in Table 2. In all cases, there is no time-lag for crystallization on the surface, which correlates with direct observation – crystallization starts on the surface immediately.

Table 2 Values of parameters describing crystallization of $Sb_{0.5}Se_{99.5}$ samples studied at given temperature where $N_{S,V}$ is the number of particles on the surface or in the volume (in number of particles per mm^2 or mm^3), $u_{S,V}$ (in m s^{-1}) is the crystal growth rate on the surface or in the volume, and τ_V is the time-lag for crystals growing in the volume of the sample.

Temperature	Surface		Volume		
(°C)	$\ln N_S$	$\ln u_S$	$\ln N_V$	$\ln u_V$	τ_V (s)
97	7.53	-17.887	11.45	-17.685	2000
102	8.80	-17.647	11.54	-17.423	950
105	8.22	-17.296	11.60	-17.014	950
110	9.11	-17.157	11.66	-17.151	400
117	9.14	-16.805	11.73	-16.928	200

As can be seen very close values of *u* can be used on the surface and in the volume of the samples to calculate DSC curves and the value of *u* increases with increasing temperature. The number of particles *N* increases with increasing temperature but the change of its value is more significant for the surface crystallization. The time-lag significantly decreases with increasing temperature of annealing and the value of time-lag for temperature of 105 °C is consistent with microscopy results where no crystals in the volume were observed up to 15 minutes of annealing. The comparison of calculated curves and experimental results is depicted in Figures 1 and 2. It must be emphasized that these are the optimal fits of the whole set and that is why the calculated curves do not perfectly fit the data. The main reason is the time-lag used for fitting the whole set. When the best fit of only one curve is done (example is in Figures 3b and 4b), it is evident that the time-lag significantly decreases with decreasing particle sizes at each temperature and is very low for particle size of 20–50 μm annealed at higher temperatures. This very short time-lag is a

reason why these DSC curves can be described by combination of two JMA curves, although the second process has unreally high values of parameter *n* (as was discussed above). The results for the best fit of only one curve reveal that parameters for surface crystallization, N_S and u_S, significantly increase with decreasing particle size at given temperature, which correlate with increasing surface/volume ratio. In the case of volume crystallization, the value of N_V slightly increases with decreasing particle size except decrease of the value for particle size of 125–180 μm. Similar trend was observed for parameter u_V except increase of the value for particle size of 125–180 μm. These trends in obtained parameters correlate with expected change in the relative proportion of surface/volume crystallization with particle sizes. As is depicted in Figure 3b, the dominant mechanism for bulk sample is the volume crystallization (deconvoluted peak for volume crystallization is significantly bigger than the peak for surface crystallization). Whereas, the Figure 4b shows that the dominant mechanism for particle size of 20–50 μm is the surface crystallization. It seems that the particle size of 125–180 μm has the ratio of surface/volume crystallization close to one, thus the deconvoluted peaks have similar sizes and the time-lag shift caused that the DSC data shows almost separated peaks with similar height (see Figure 1a and 2b).

Noticing these trends in parameters with particle sizes, it is obvious that fitting the set of data for one temperature and different particle sizes at ones cannot provide perfect fit of all the data but give rough determination of parameters for surface and volume crystallization, which can be compared with results for other temperature.

Evaluating the proposed procedure of calculation of DSC curves based on nucleation and growth rates, it must be pointed out that the assumptions of the concept are very simple. For example, the shape of bulk sample has nothing to do with the sphere, but it is a thin plate with the thickness of 1 mm. Even though the proposed concept is the simplest model of sample and crystals, it can explain complex shapes of DSC curves and their changes with particle sizes. This model and its parameters can explain the changes of dominant mechanism for complex surface/volume crystallization with particle size.

Focusing on crystals growth rates, the values obtained from DSC data fitting (shown in Table 2) are higher compared to growth rates in pure selenium[4,40]. Thus, we can conclude that a small addition of antimony into selenium accelerates the overall crystallization process in comparison with pure selenium.

Conclusion

Crystallization studies done by DSC can be affected strongly by particle size of the sample when the process consists of crystallization on the surface and in the volume, and surface/volume ratio can play the key role. Thus, care must be taken to sample preparation and testing of samples with different particle sizes is recommended. Studied $Sb_{0.5}Se_{99.5}$ composition is a perfect example of the complex crystallizing system with crystals growing on the surface joined by postponing growth of the crystals in the volume. The time-lag of volume crystallization caused that the standard kinetic models cannot describe all the experimental data. The simple model, based on nucleation and growth processes on the surface and in the volume, can explain huge difference in the shape of DSC curves with particle sizes.

Acknowledgement

This work has been supported by the Czech Science Foundation under project No. 16-10562S.

References

(1) Elliott, S.R. Chalcogenide glasses. In *Material Science Technology*; Wiley-VCH Verlag GmbH & Co. KGaA: Weinheim, 2006.
(2) Mikla, V. I.; Mikhalko, I. P.; Nagy, Y. Y.; Mateleshko A.V.; Mikla V. V. Electronic properties of Sb_xSe_{1-x} glasses. *J Mat Sci.* **2000**, 35, 4907-4912.
(3) Kržmanc, M. M.; Došler, U.; Suvorov, D. The nucleation and crystallization of MgO-B_2O_3-SiO_2 glass, *J. Eur. Ceram. Soc.* **2011**, 31, 2211-2219.
(4) Ryschenkow, G.; Faivre, G. Bulk crystallization of liquid selenium. Primary nucleation, growth kinetics and modes of crystallization, *J. Cryst. Growth* **1988**, 87, 221-235.
(5) Yuryev, Y.; Wood-Adams, P. Effect of surface nucleation on isothermal crystallization kinetics: Theory, simulation and experiment, *Polymer* **2011**, 52, 708-717.
(6) Barták, J.; Martínková, S.; Málek, J. Crystal growth kinetics in Se-Te bulk glasses, *Cryst. Growth Des.* **2015**, 15, 4287-4295.
(7) Ray, C. S.; Fang, X.; Day, D. E. New method for determining the nucleation and crystal-growth rates in glasses. *J. Am. Ceram. Soc*. **2000**, 83, 865-872.
(8) Fokin, V.M.; Yuritsyn, N. S.; Zanotto, E. D.; Schmelzer, J. W. P.; Cabral, A. A. Nucleation time-lag from nucleation and growth experiments in deeply undercooled glass-forming liquids, *J. Non-Cryst. Solids* **2008**, 354, 3785-3792.
(9) Zmrhalová, Z.; Pilný, P.; Svoboda, R.; Shánělová, J.; Málek, J. Thermal properties and viscous flow behavior of As_2Se_3 glass, *J. All. Comp*. **2016**, 655, 220-228.

(10) Málek, J. Kinetic analysis of crystallization processes in amorphous materials, *Thermochim. Acta* **2000**, 355, 239-253.
(11) Johnson, W. A.; Mehl, K. F. Reaction kinetics in processes of nucleation and growth. *Trans. Am. Inst. Min. Metall. Eng.* **1932**, 135, 416–442.
(12) Avrami, M. Kinetics of phase change I – general theory. *J. Chem. Phys.* **1939**, 7, 1103–1112.
(13) J. W. Christian, The theory of transformations in metals and alloys, 2nd Ed., Pergamon Press, New York 1975, p. 525
(14) Henderson, D.W. Thermal analysis of non-isothermal crystallization kinetics in glass forming liquids. *J. Non-Cryst. Solids* **1979**, 30, 301-315.
(15) Shepilov, M.P.; Baik, D.S. Computer-simulation of crystallization kinetics for the model with simultaneous nucleation of randomly-oriented ellipsoidal crystals. *J. Non-Cryst. Solids* **1994**, 171, 141-156.
(16) Málek, J.; Mitsuhashi, T. Testing method of the Johnson-Mehl-Avrami equation in kinetic analysis of the crystallization processes, *J. Am. Ceram. Soc*. **2000**, 83, 2103-2105.
(17) Fraser, R.D.B.; Suzuki, E. Resolution of overlapping bands. Function for simulating band shapes. *Anal. Chem.* **1969**, 41, 37-39.
(18) Perejón, A.; Sánchez-Jiménez, P.E.; Criado, J.M.; Pérez-Maqueda, L.A. Kinetic analysis of complex solid-state reactions. A new deconvolution procedure. *J. Phys. Chem. B* **2011**, 115, 1780-1791
(19) Svoboda, R.; Málek, J. Applicability of Fraser-Suzuki function in the kinetic analysis of complex crystallization processes. *J. Therm. Anal. Cal.* **2013**, 111, 1045-1056.
(20) Liška, M.; Holubová, J.; Černošková, E.; Černošek, Z.; Chromčíková, M.; Plško, A. Nucleation and crystallization of an As_2Se_3 undercooled melt. *Phys. Chem. Glasses: Eur. J. Glass Sci. Technol. B* **2012**, 53, 289-293.
(21) Honcová, P.; Pilný, P.; Svoboda, R.; Shánělová, J.; Koštál, P.; Barták, J.; Málek, J. Analysis of crystallization in Sb_2Se_{98} composition, *J. Therm. Anal. Cal.* **2014**, 116, 613-618.
(22) Moharram, A.H.; Abu El-Oyoun, M.; Rashad, M. Crystallization kinetics of two overlapped phases in $As_{40}Te_{50}In_{10}$ glass, *Thermochim. Acta* **2013**, 555, 57-63.
(23) El-Zaidia, M. M.; El-Shafi, A.; Ammar, A. A.; Abo-Ghazala, M. Physical properties and structural studies of $Se_{100-x}Sb_x$, *Thermochim. Acta* **1987**, 116, 35-44.
(24) Mehta, N.; Kumar, A. Observation of phase separation in some Se-Te-Ag chalcogenide glasses, *Mat. Chem. Phys*. **2006**, 96, 73-78.
(25) Othman, A. A.; Amer, H. H.; Osman, M. A.; Dahshan, A. Non-isothermal crystallization kinetics study on new amorphous $Ga_{20}Sb_5S_{75}$ and $Ga_{20}Sb_{40}S_{40}$ chalcogenide glasses, *J. Non-Cryst. Solids* **2005**, 351, 130-135.
(26) Abdel-Rahim, M. A.; Hafiz, M. M.; Mahmoud, A. Z. Crystallization kinetics of overlapping phases in $Se_{70}Te_{15}Sb_{15}$ using isoconversional methods, *Prog. Nat. Sci. Mat. Int.* **2015**, 25, 169-177.
(27) Moharram, A. H.; Abu El-Oyoun, M.; Rashad, M. Crystallization kinetics of two overlapped phases in $As_{40}Te_{50}In_{10}$ glass, *Thermochim. Acta* **2013**, 555, 57-63.
(28) Abdel-Rahim, M. A.; El-Korashy, A.; Hafiz, M. M.; Mahmoud, A. Z. Kinetic study of non-isothermal crystallization of Bi_xSe_{100-x} chalcogenide glasses, *Phys. B* **2008**, 403, 2956-2962.

(29) Svoboda, R.; Málek, J. Crystallization kinetics of a-Se. Part 3. Isothermal data, *J. Therm. Anal. Cal.* **2015**, 119, 1363-1372.
(30) Holubová, J.; Černošek, Z.; Černošková, E. The selenium based chalcogenide glasses with low content of As and Sb: DSC, StepScan DSC and Raman spectroscopy study, *J. Non-Cryst. Solids* **2009**, 355, 2050-2053.
(31) Tonchev, D.; Kasap, S.O. Thermal properties of Sb_xSe_{1-x} glasses studied by modulated temperature differential scanning calorimetry, *J. Non-Cryst. Solids* **1999**, 248, 28-36.
(32) Mehta, N.; Zulfequar, M.; Kumar, A. Kinetic parameters of crystallization in glassy $Se_{100-x}Sb_x$ alloys, *Phys. Stat. Sol*. **2005**, 203, 236-246.
(33) Pilný, P. OriTas program – solution for kinetic analysis of thermoanalytical data. http://www.petrpilny.cz/oritasen. Accessed 20 Jan 2015
(34) Ghosh, G.; Lukas, H. L.; Delaey, L. A thermodynamic assessment to the Sb-Se system. *Z. Metallkunde* **1989**, 80, 663-668.
(35) Berkes, J. S.; Myers, M. B. Phase relations and liquid structure in the system As-Sb_2Se_3-Se, *J. Electrochem. Soc.* **1971**, 118, 1485-1491.
(36) Svoboda, R.; Málek, J. Crystallization kinetics of amorphous Se, part 1 – interpretation of kinetic functions. *J. Therm. Anal. Cal*. **2013**, 114, 473-482.
(37) Svoboda, R.; Málek, J. Crystallization kinetics of amorphous Se, part 2 – Deconvolution of a complex proces: the final answer. *J. Therm. Anal. Cal*. **2014**, 115, 81-91.
(38) Svoboda, R.; Málek, J. Crystallization kinetics of amorphous Se, part 3 – Isothermal data, *J. Therm. Anal. Cal*. **2015**, 119, 1363-1372.
(39) Pustková, P.; Zmrhalová, Z.; Málek, J. The particle size influence on crystallization kinetics of $(GeS_2)_{0.1}(Sb_2S_3)_{0.9}$ glass. *Thermochim. Acta* **2007**, 466, 13–21.
(40) Barták, J. Crystallization kinetics in undercooled chalcogenide systems. PhD Dissertation, University of Pardubice, Pardubice, 2014.